

EUROPEAN SOUTHERN OBSERVATORY VERY LARGE TELESCOPE OPTICAL SPECTROSCOPY OF BL LACERTAE OBJECTS. III. AN EXTENSION OF THE SAMPLE

B. SBARUFATTI¹, S. CIPRINI^{2,3}, J. KOTILAINEN³, R. DECARLI⁴, A. TREVES⁴, A. VERONESI⁴, AND R. FALOMO⁵

¹ INAF, Istituto di Astrofisica Spaziale e Fisica Cosmica di Palermo, Via Ugo La Malfa 153, I-90146 Palermo, Italy; sbarufatti@ifc.inaf.it

² Physics Department University of Perugia, and I.N.F.N. Perugia Section, Via A. Pascoli, I-06123 Perugia, Italy

³ Tuorla Observatory, University of Turku, Väisäläntie 20, FIN-21500 Piikkiö, Finland

⁴ Università dell'Insubria, Via Valleggio 11, I-22100 Como, Italy

⁵ INAF, Osservatorio Astronomico di Padova, Vicolo dell'Osservatorio 5, I-35122 Padova, Italy

Received 2008 May 13; accepted 2008 October 20; published 2008 December 15

ABSTRACT

We present results of an ongoing program at the European Southern Observatory Very Large Telescope for spectroscopy of BL Lac objects (BLLs) lacking a firm redshift estimate, and here we report on 15 objects. For 11 sources we confirm the BL Lac classification, and determine new redshifts for three objects, one with weak emission lines (PKS 1057 – 79, $z = 0.569$) and two with absorptions from the host galaxy (RBS 1752, $z = 0.449$; RBS 1915, $z = 0.243$); moreover, a subdamped Ly α system is detected in the direction of the BL Lac PKS 0823 – 223 ($z \geq 0.911$). For the remaining eight BLLs, from the very absence of absorption lines of the host galaxy, lower limits to the redshift are deduced with z_{\min} in the interval 0.20–0.80. The remaining three sources are reclassified as a FSRQ (PKS 1145 – 676, $z = 0.210$; TXS 2346+052, $z = 0.419$) and a misclassified galactic star (PMNJ 1323 – 3652).

Key word: BL Lacertae objects: general

1. INTRODUCTION

Blazars dominate the scene of extragalactic gamma-ray astronomy, as space-borne missions and Cerenkov atmospheric telescopes have shown. BL Lac objects (BLLs) are a main subclass of blazars that by definition exhibit featureless spectra or very weak lines, most probably because of the relativistic enhancement of the continuum. Surely, the recent launch of *AGILE* and *GLAST* gamma-ray observatories and the upgrading of the existing ground-based Cerenkov telescopes will significantly increase the interest in the BLLs. The determination of the redshift is mandatory in order to characterize these sources (e.g., to determine the nuclear and host galaxy luminosity of the sources), but it is arduous, in most of the objects, to detect the weak spectral features over the continuum. Indeed, a redshift determination exists for only about half of the known BLLs. The detection of the weak spectral lines necessarily requires the use of 8–10 m telescopes. In addition to the issue of redshift, high signal-to-noise ratio (S/N) and spectral resolution are also of importance for detecting the host galaxy independently of imaging, since its emission may appear superposed to the non-thermal continuum of the nucleus. Absorption lines may be related to the host galaxy itself, to the intergalactic medium, and to the interstellar medium (ISM) of our Galaxy and its halo. The emission lines are the most direct probe to the physical conditions around the nucleus.

We have an ongoing program for BL Lac's spectroscopy at the European Southern Observatory (ESO) 8 m Very Large Telescope (VLT), which utilizes the telescope in service mode under nonoptimal seeing conditions. The results of the first three runs (2003 and 2004) referred to 35 BLLs. We measured new redshifts for 17 sources, while for the rest of the objects we have given upper limits using a technique specifically designed for this project. Details are given in Sbarufatti et al. (2005b, 2006b, hereafter S05 and S06, respectively), together with the criteria on the sample selection.

In this paper we present the spectra of 15 objects observed in 2006 (Guest Observer run: ESO 077.B-0045). Data reduction

and analysis procedures are described in Section 2. Results are reported in Section 3 along with specific comments about each source. The summary and conclusion are given in Section 4. Throughout this paper we assume the following cosmological parameters: $H_0 = 70 \text{ km s}^{-1} \text{ Mpc}^{-1}$, $\Omega_\Lambda = 0.7$, and $\Omega_m = 0.3$.

2. OBSERVATIONS AND DATA ANALYSIS

The observations (Table 1) were performed between 2006 March and 2006 August in Service Mode at the ESO VLT UT2 (Kueyen) telescope, equipped with the FOcal Reducer and low-dispersion Spectrograph (FORIS1), using the 300V+I grism combined with a 2'' slit, yielding a dispersion of 112 \AA mm^{-1} (corresponding to $2.64 \text{ \AA pixel}^{-1}$) and a spectral resolution of 15 \AA covering the 3800–8000 \AA range. The seeing during observations was in the range 0'.5–2'.5, with an average of 1''.

We performed data reduction using IRAF⁶ (Tody 1986, 1993), following the standard procedures for spectral analysis. This includes bias subtraction, flat fielding, and removal of bad pixels. For each target, we obtained three spectra for an optimal correction of the cosmic rays and to check for the reality of weak spectral features. The individual frames were then combined into a single average image. Wavelength calibration was performed using the spectra of a He/Ne/Ar lamp, resulting in an accuracy of $\sim 3 \text{ \AA}$ (rms). From these calibrated final images, we extracted the one-dimensional spectra inside a 2'' \times 6'' aperture, adopting an optimal extraction algorithm (Horne 1986) to improve the S/N.

As a part of a fill-in program, our observations did not require optimal photometric conditions. However, the sky was clear for most of the observations. This enabled us to perform a spectrophotometric calibration of the data using standard stars (Oke 1990). We estimate an uncertainty of the order of 10% in the flux calibration because of the nonoptimal sky

⁶ IRAF is distributed by the National Optical Astronomy Observatories, which are operated by the Association of Universities for Research in Astronomy, Inc., under cooperative agreement with the National Science Foundation.

Table 1
Journal of Observations

Object Name	IAU Name	R.A. (J2000)	Decl. (J2000)	Date of Obs.	Exposure (s)	S/N	EW _{min} (Å)	z
(1)	(2)	(3)	(4)	(5)	(6)	(7)	(8)	(9)
PKS 0019+058	0019+058	00 22 32	+06 08 04	Jul 12	2400	120	0.38	> 0.49
...	Aug 8	2400	70	0.40	> 0.64
GC 0109+224	0109+224	01 12 06	+22 44 39	Sep 1	4065	380	0.09	> 0.25
RBS 0231	None	01 40 41	-07 58 49	Jul 13	2400	20	1.27	> 0.41
PKS 0823-223	0823-223	08 26 02	-22 30 27	Apr 14	2400	220	0.41	≥ 0.911
PKS 1057-79	1057-797	10 58 43	-80 03 54	Mar 31	2400	90	0.39	> 0.581
PKS 1145-676	1145-676	11 47 33	-67 53 42	Apr 14	2400	80	1.84	0.210
OM 280	1147+245	11 50 19	+24 17 54	Apr 16	2400	100	0.35	> 0.20
PMN J1323-3652	None	13 23 46	-36 53 39	May 7	2400	20	1.57	0
OQ 012	1407+022	14 10 04	+02 03 07	May 7	2400	120	0.31	> 0.63
PMNJ 1539-0658	None	15 39 10	-06 58 43	Mar 28, Apr 20	4800	50	0.61	> 0.80
PKS 1830-589	1830-589	18 34 28	-58 56 36	Apr 15	2400	100	0.46	> 0.45
RBS 1752	None	21 31 35	-09 15 23	May 10	2400	90	0.49	0.448
RBS 1915	None	22 56 13	-33 03 38	May 5	2400	160	0.35	0.243
TXS 2346+052	2346+052	23 49 21	+05 34 40	Jul 1	2400	80	0.63	0.419
1RXS J235730.1-171801	None	23 57 30	-17 18 05	Jul 1	2400	110	0.22	> 0.63

Notes. Description of columns: (1) object name; (2) IAU J1950 code name; (3) right ascension (J2000); (4) declination (J2000); (5) date of observations, year 2006; (6) exposure time; (7) signal-to-noise ratio; (8) minimum-detectable EW, calculated following Sbarufatti et al. (2006b); (9) redshifts measured from spectral features and redshift lower limits.

condition. Flux losses due to the slit not being oriented along the parallactic angle are negligible with respect to the flux-calibration uncertainties. All of the spectra were dereddened following the extinction law by Cardelli et al. (1989) and assuming the E_{B-V} values computed by Schlegel et al. (1998).

3. RESULTS

In Figure 1 we give the optical spectrum for each source. In order to make apparent the shape of the continuum and the faint spectral features, we report both the flux-calibrated and the normalized spectra. Intrinsic and intervening spectral features are identified with atomic species. Absorptions caused by the Galactic interstellar medium are indicated with ISM for simple atomic species, and with diffuse interstellar band (DIB) for complex molecules. The Earth symbol is used to mark telluric absorptions. All spectra can be retrieved in electronic form at <http://www.oapd.inaf.it/zbllac/>, where all the results of our program are archived.

3.1. Continuum Emission and Host Galaxy Contribution

The optical spectrum of a BLL can be described, in a first approximation, as the superposition of two components. The first one is a non-thermal continuum emitted by the active nucleus. The second is the contribution from the stars and the ISM of the BLL host galaxy. Extensive studies in the past (e.g., Urry et al. 2000) have shown that these galaxies are usually giant ellipticals, the optical magnitudes of which follow a narrow Gaussian distribution centered around $M_R^{\text{host}} = -22.9 \pm 0.5$ (Sbarufatti et al. 2005a). In most cases the host galaxy signature was not detected in our spectrum because it was too faint with respect to the nuclear component. For these objects, we performed a fit of the optical continuum with a simple power-law model ($F_\lambda \propto \lambda^{-\alpha}$). In two cases however (RBS 1752 and RBS 1915) the host galaxy spectral features were detected, and we performed a fit to the spectrum using a two-component model (see Figure 2): a power-law plus an elliptical galaxy spectrum as in the template given in Kinney et al. (1996; also see S06 for details on the fitting procedure). The results from

Table 2
Spectral Fits

Object Name	α	M_R^{host}	Class	R	E_{B-V}	References
(1)	(2)	(3)	(4)	(5)	(6)	(7)
PKS 0019+058	-0.65		L	17.7	0.023	N96, G00
PKS 0019+058	-0.76		L	18.4	0.023	N96, G00
GC 0109+224	-0.82		L	14.6	0.049	N96, W07
RBS 0231	-1.00		L	18.6	0.109	G05
PKS 0823-223	-0.47		H	15.4	0.472	D90, W92
PKS 1057-79	-0.73		L	15.9	0.306	F04, E04
OM 280	-0.79		L	15.7	0.027	D01, G95
OQ 012	-0.29		L	18.1	0.108	N06
PMNJ 1539-0658	-0.50		L	19.5	0.156	L01
PKS 1830-589	-0.65		L	17.7	0.095	L01
RBS 1752	-1.45	-23.3	L	17.5	0.037	G05
RBS 1915	-1.09	-22.4	L	16.8	0.018	B00
TXS 2346+052	-0.06		L ^a	18.3	0.187	V05
1RXS J235730.1-171801	-1.40		H	17.7	0.070	G05

Notes.

(1) Object name; (2) spectral index of the continuum, α , defined by $F_\lambda \propto \lambda^{-\alpha}$; (3) absolute R magnitude of the host galaxy; (4) class of the object (H: high-energy peaked BLL; L: low-energy peaked BLL); (5) apparent R magnitude of the object, extracted within a $6'' \times 2''$ aperture; (6) Galactic extinction in the direction of the object, from Schlegel et al. (1998). (7) References for HBL/LBL classification: D90: della Ceca et al. (1990), W92: White (1992), G95: Ghosh & Soundararajaperumal (1995), N96: Nass et al. (1996), B00: Bauer et al. (2000), G00: Gorshkov et al. (2000), D01: Donato et al. (2001), L01: Landt et al. (2001), E04: Edwards & Tingay (2004), F04: Fleisch & Hardcastle (2004), G05: Giommi et al. (2005b), V05: Vollmer et al. (2005), N06: Nieppola et al. (2006), and W07: Wu et al. (2007).

^a Source lacking an X-ray detection in the literature. The LBL classification is tentative.

our fits are reported in Table 2, where for each object we give the power-law index, the object class (High-Energy Peaked BLL, HBL; Low-Energy Peaked BLL, LBL; see Padovani & Giommi 1995 for a definition), the apparent magnitude, and the extinction coefficient. For RBS 1752 and RBS 1915, we also report the absolute magnitudes of the host galaxies corrected for the aperture effects, which were $M_R = -23.3$ and -22.4 , respectively, in agreement with the expected distribution.

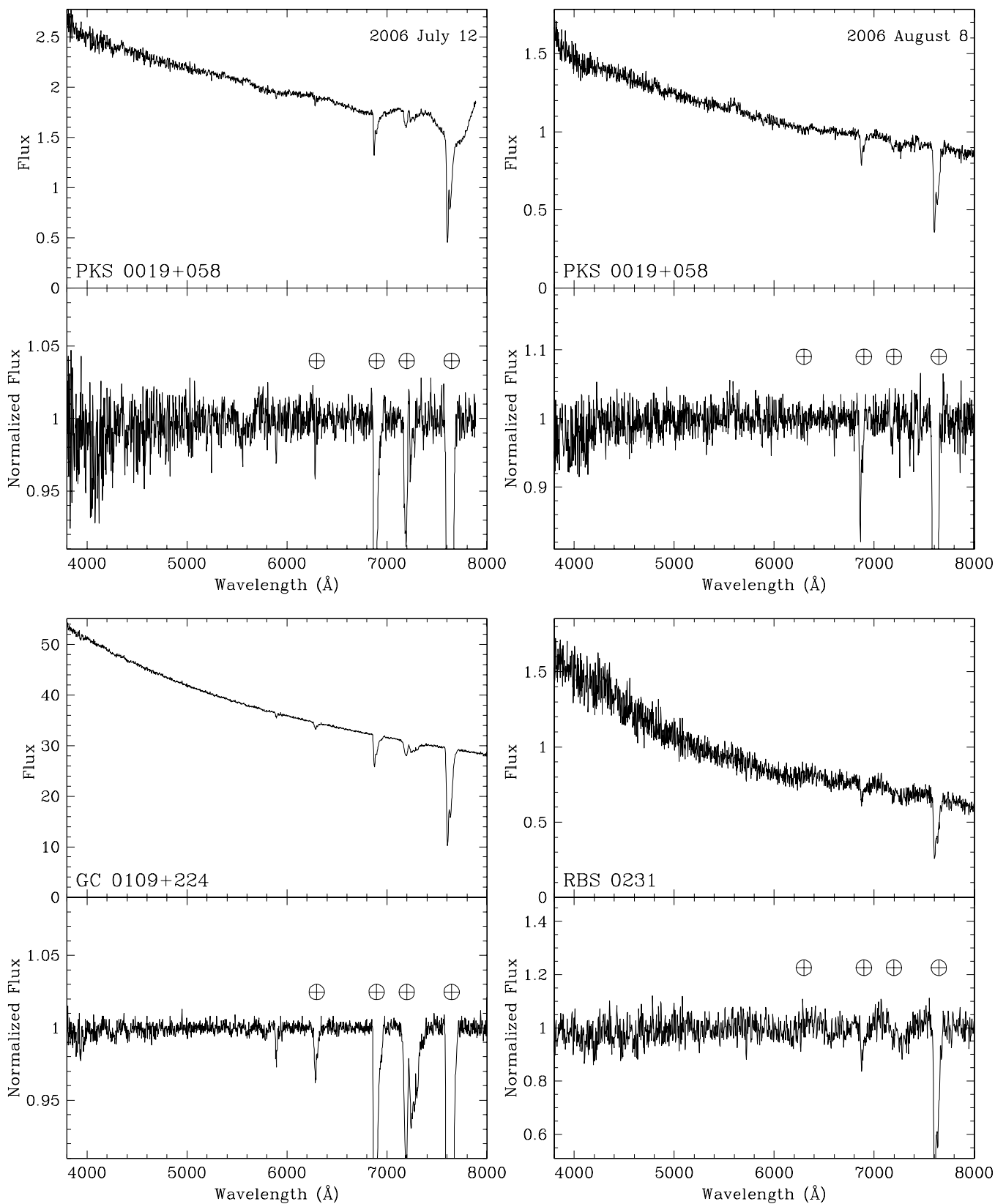


Figure 1. Spectra of the observed objects. Top panels: flux-calibrated dereddened spectra. Bottom panels: normalized spectra. Telluric bands are indicated by ⊕, spectral lines are marked by the line identification, absorption features from atomic species in the interstellar medium of our Galaxy are labeled by ISM, and diffuse interstellar bands by DIB. The flux density is given in units of $10^{-16} \text{ erg cm}^{-2} \text{ s}^{-1} \text{ \AA}^{-1}$.

3.2. Line Detection and Redshift Determination

Since emission and absorption lines in a BLL spectrum can be very faint, their detection can be a difficult task. Using the

same technique presented in S06, we estimated the minimum detectable equivalent width, EW_{\min} , for each spectrum, and considered all features with equivalent width (EW) above this

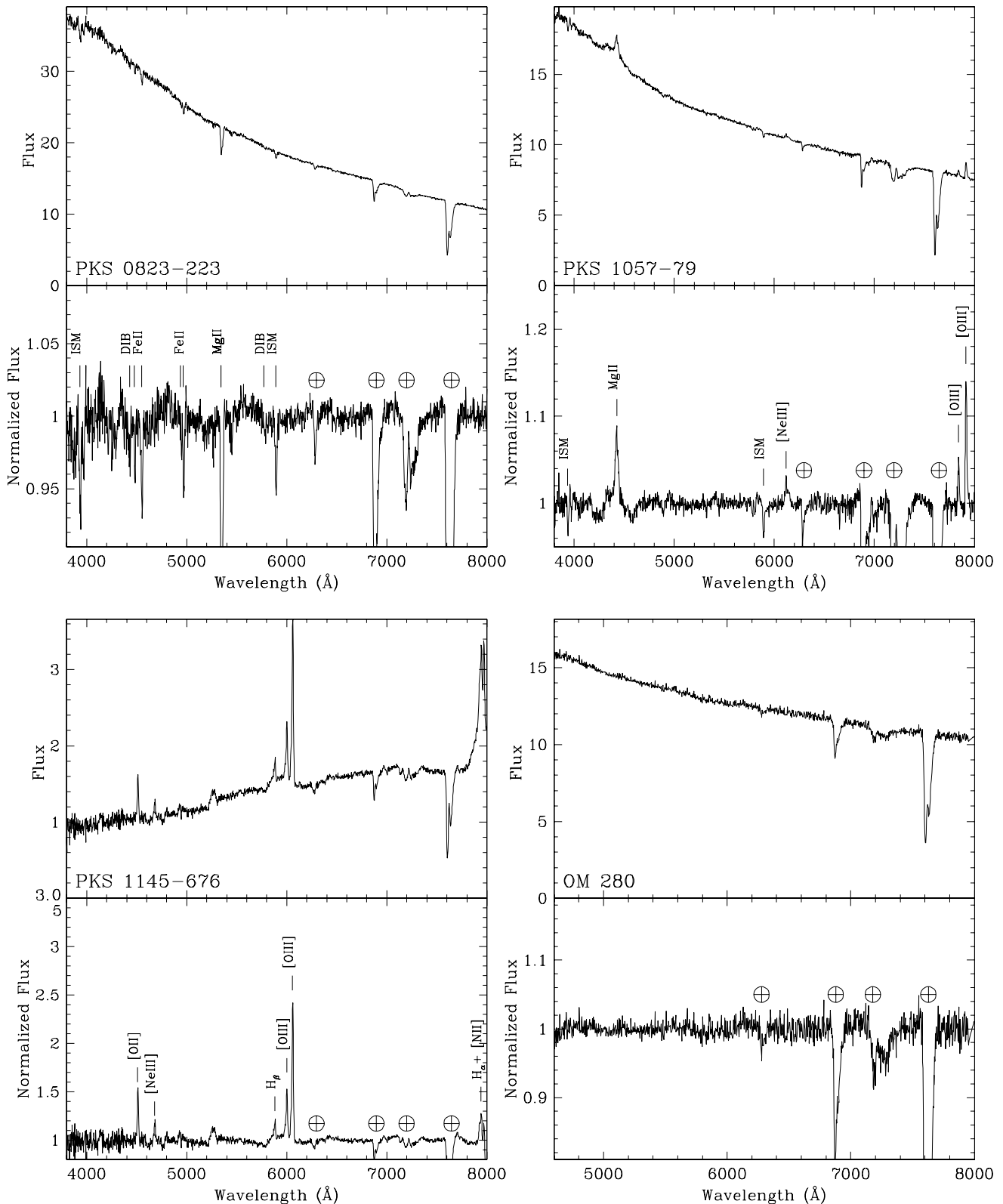


Figure 1. (Continued)

threshold as line candidates which were then carefully inspected for identification or rejection. EW_{\min} values for each spectrum are given in Table 1, while line identifications, full width at half-maximum (FWHM), and EW are reported in Table 3. The continuum and line properties confirmed the BL Lac classification for 12 objects. In Section 3.3 we report notes on the individual sources.

3.2.1. Redshift Lower Limits

Most of the confirmed BLLs in our sample show featureless spectra, despite the high S/N reached using VLT. As extensively discussed in S06 (in Section 4.2.4), it is possible to estimate a lower limit to the redshift of such sources, knowing the EW_{\min} and the nucleus apparent magnitude, and exploiting the

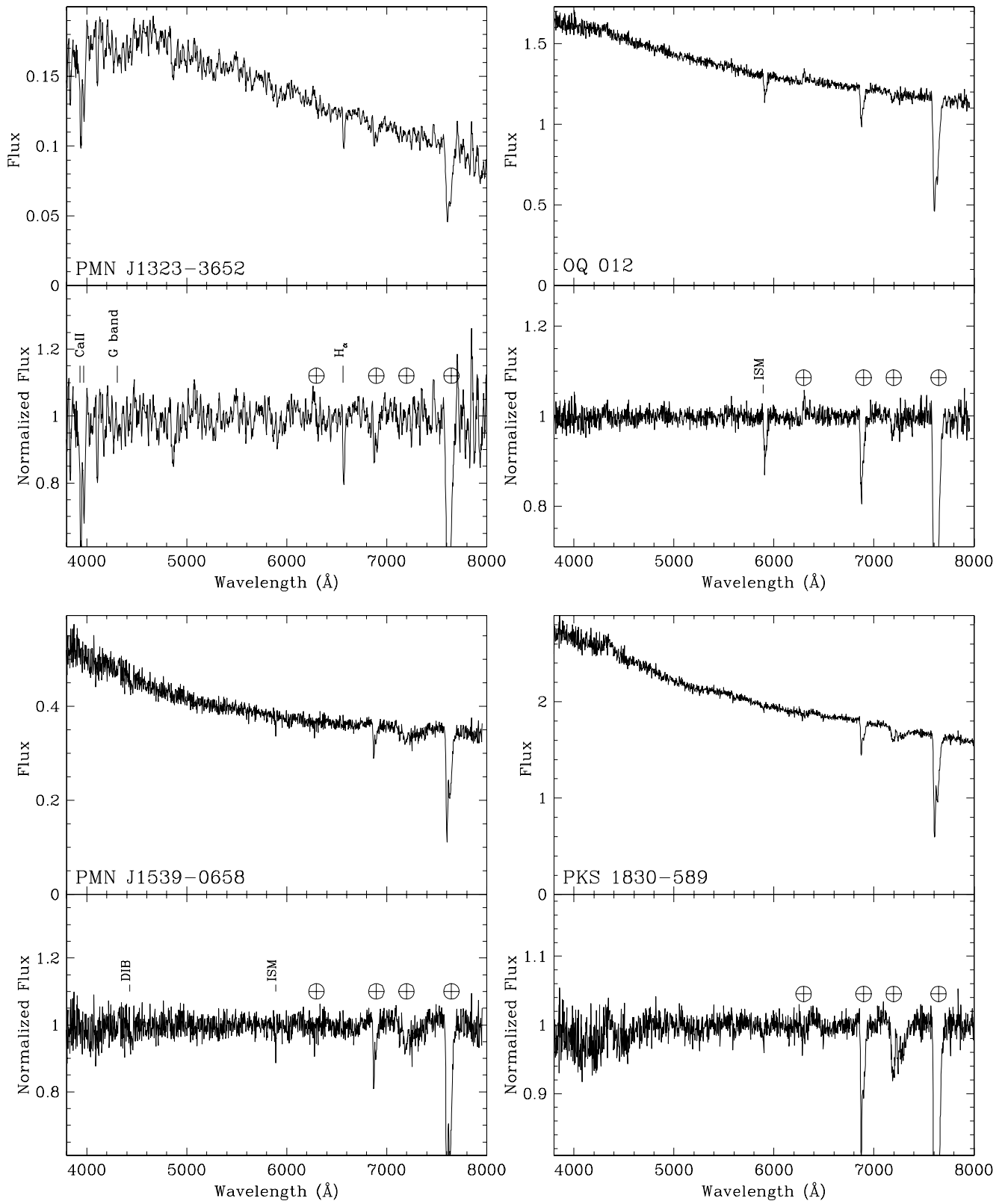


Figure 1. (Continued)

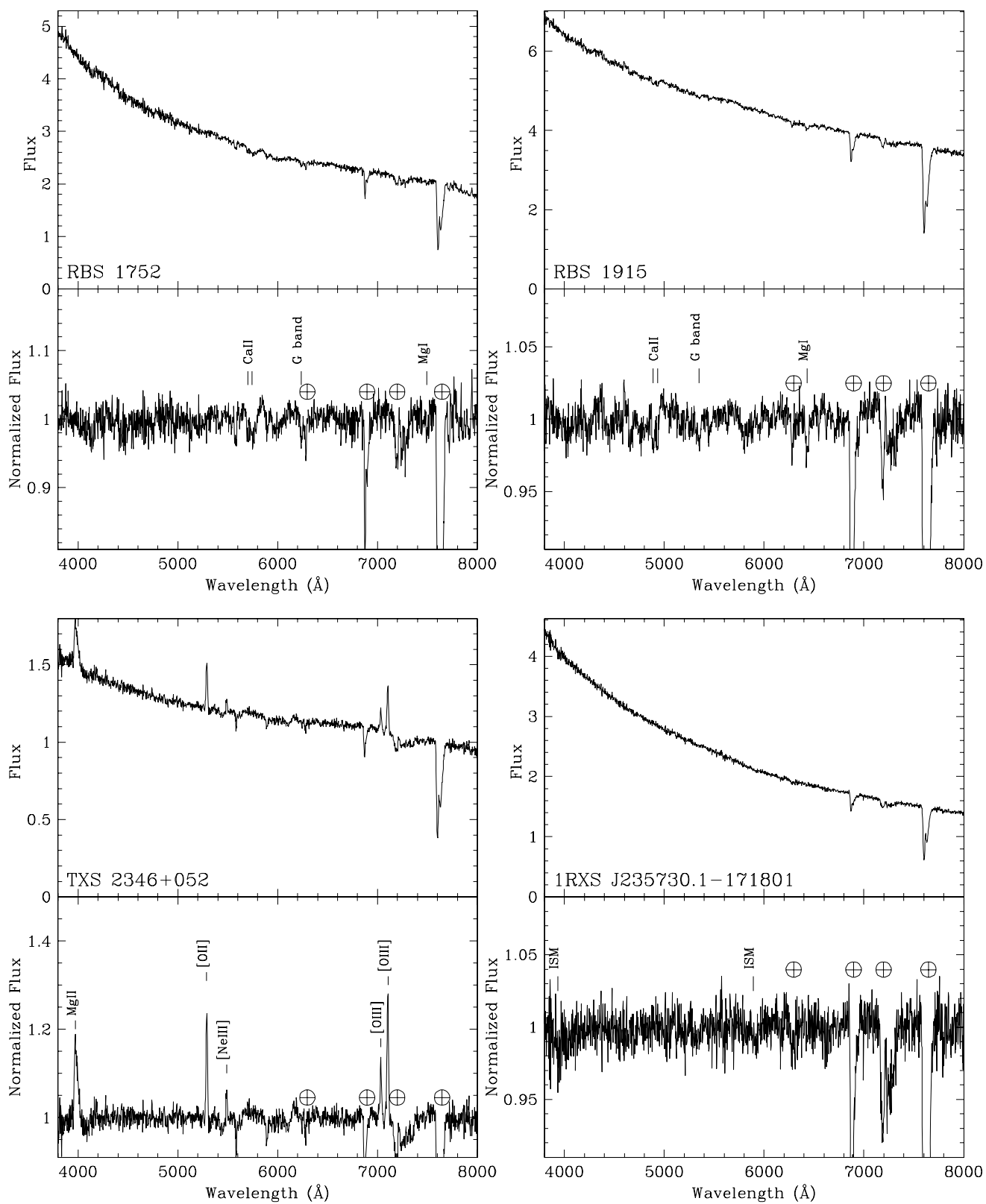


Figure 1. (Continued)

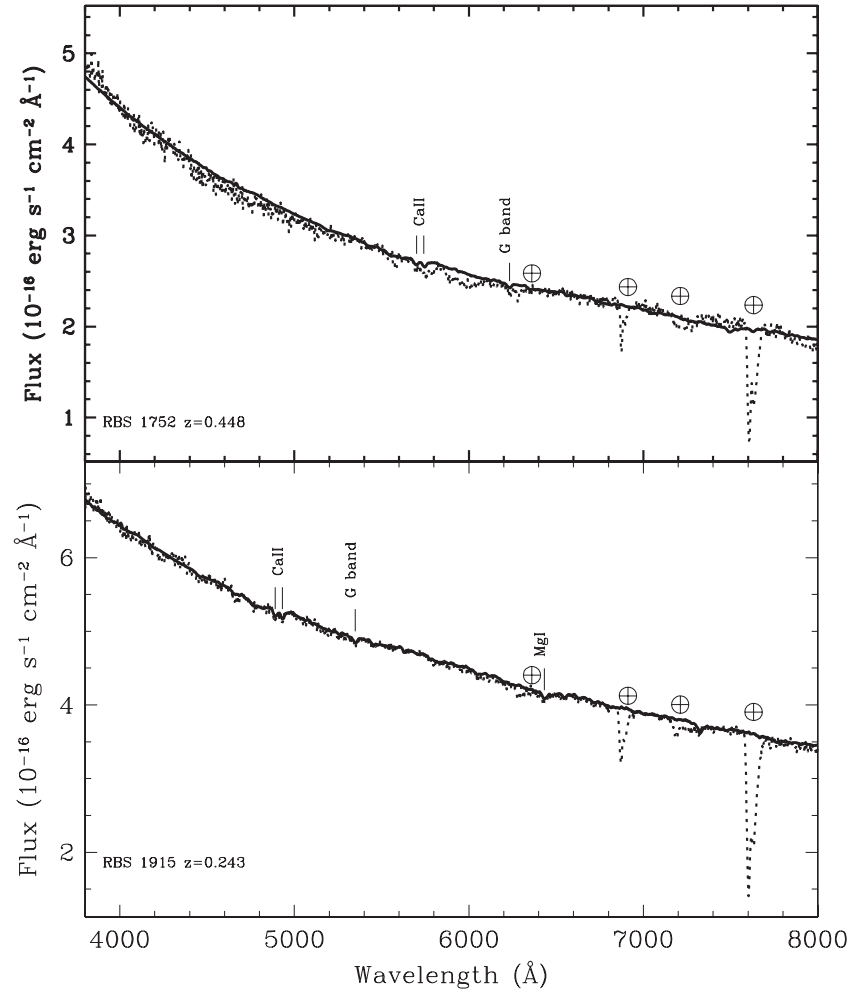


Figure 2. Spectral decomposition for objects RBS 1752 and RBS 1915. Solid line shows the fitted spectrum, while dotted line shows the observed one.

assumption that BL Lac hosts can be considered as candles (Sbarufatti et al. 2005a). We remark here that Equation (1) in S06 contains a typographical error, which was noted also by Finke et al. (2008). The correct expression is

$$EW_{\text{obs}} = \frac{(1+z) \times EW_0}{1 + \rho/A(z)}, \quad (1)$$

where EW_{obs} is the observed equivalent width, EW_0 is the equivalent width of the feature in the host galaxy template (Kinney et al. 1996), ρ is the nucleus-to-host flux ratio, z is the redshift, and $A(z)$ is the aperture correction.

We applied this procedure to all featureless spectra in the sample, obtaining the lower limits reported in Section 3.3.

3.3. Notes on Individual Objects

PKS 0019+058. This radio-selected source (Condon & Jauncey 1974) was first classified as a BLL by Fricke et al. (1983), based on a featureless optical spectrum. We observed this object in two epochs separated by about a month, noticing an optical variability of 0.7 mag (R band) and an evolution of the spectral index from 0.65 to 0.76. The reality of the optical variability is fully confirmed by the R -band images exposed prior to the spectra which enable direct photometry. The optical variability was known, both in magnitude ($V = 19.2$ and $V > 21$

in Fricke et al. 1983; Abraham et al. 1991, respectively) and in spectral index ($\alpha_v = 0.8$ and 0.94 in Fricke et al. 1983; Chen et al. 2005). We find no intrinsic feature with $EW > EW_{\text{min}}$ in any of the two spectra. The Na I $\lambda 5891$ absorption from the Galaxy ISM is detected in both spectra with $EW = 0.43 \text{ \AA}$ (July 12) and 0.66 \AA (August 8). A marginally significant excess around 5600 \AA is present in both observations, but it is most probably spurious because of residuals left after the subtraction of a nearby atmospheric emission line. The most stringent redshift lower limit, obtained from the 2006 August spectrum, is $z > 0.64$.

GC 0109+224. This source was discovered in radio observations by Davis (1971), and subsequently classified as a BLL by Owen & Muffson (1977). Strong flux and polarization variability was reported both in the radio and optical band (e.g., Katajainen et al. 2000; Ciprini et al. 2003, 2004). Optical imaging by Falomo (1996) and Nilsson et al. (2003) failed to detect the host galaxy, while the detection reported by Wright et al. (1998) is dubious, since it has not been confirmed by any subsequent observation. The lower limit on the redshift proposed by Falomo (1996) is $z > 0.4$. Previous optical spectroscopy by Wills & Wills (1979), Falomo et al. (1994), and Sbarufatti et al. (2006a) performed with 2–4 m class telescopes showed featureless spectra, while Healey et al. (2008) report $z = 0.265$ for this object based on an unpublished optical spectrum. The

Table 3
Spectral Lines

Object Name	Object Class	z	Line ID	Wavelength (\AA)	z_{line}	Type	FWHM (km s^{-1})	EW (\AA)
(1)	(2)	(3)	(4)	(5)	(6)	(7)	(8)	(9)
PKS 0823–223	Sub-DLA/BLL	≥ 0.911	Galactic Ca II K	3935	0	i	1700	1.85
			Galactic Ca II H	3970	0	i	1500	1.00
			Fe II	4481	0.911	a	800	0.47
			Fe II	4553	0.911	a	1300	1.33
			Fe II	4948	0.914	a	600	0.30
			Fe II	4970	0.912	a	800	0.85
			Mg II	5349	0.911	a	1300	4.12
			Mg I	5452	0.911	a	600	0.44
			Galactic Na I	5893	0	i	900	1.08
PKS 1057–79	BLL	0.581	Mg II	4423	0.581	e	3400	–4.24
			Ne III	6119	0.582	e	300	–0.25
			[O III]	7842	0.581	e	500	–1.25
			[O III]	7917	0.581	e	500	–3.58
PKS 1145–676	QSO	0.210	[O II]	4512	0.210	e	1000	9.25
			[Ne III]	4680	0.210	e	1200	3.99
			H β	5880	0.210	e	900	5.52
			[O III]	6001	0.210	e	1000	9.14
			[O III]	6059	0.210	e	800	24.66
			H α	7944	0.210	e
			N II	7970	0.210	e
RBS 1752	BLL	0.448	Ca II	5693	0.447	g	1000	0.5
			Ca II	5749	0.449	g	1900	0.9
			G-band	6237	0.449	g	1200	1.0
			Mg I	7493	0.448	g	600	0.4
RBS 1915	BLL	0.243	Ca II	4890	0.243	g	1700	0.75
			Ca II	4932	0.243	g	1100	0.46
			G-band	5351	0.243	g	2600	0.88
			Mg I	6429	0.243	g	1900	1.96
TXS 2346+052	FSRQ	0.419	Mg II	3973	0.420	e	3600	–7.0
			[O II]	5290	0.419	e	1000	–5.0
			[Ne V]	5488	0.419	e	800	–1.2
			[O III]	7033	0.418	e	700	–2.1
			[O III]	7103	0.419	e	700	–5.3

Notes. Description of columns: (1) object name; (2) object class; (3) average redshift; (4) line identification; (5) observed wavelength of the line center; (6) redshift of the line; (7) type of the line (e: emission line, g: absorption line from the host galaxy, a: absorption line from intervening systems, and i: absorption line from our Galaxy ISM); (8) FWHM of the line; (9) EW of the line.

lower limit to the redshift as deduced by Sbarufatti et al. (2006a) was based on an $\text{EW}_{\text{min}} = 0.43 \text{ \AA}$ that yielded $z > 0.18$. The considerably higher S/N spectrum that we obtained with VLT has $\text{EW}_{\text{min}} = 0.09 \text{ \AA}$, which in turn implies $z > 0.25$, which improves the previous spectroscopical limit, but it is still less stringent than the imaging limit.

RBS 0231. This X-ray-selected object (Voges et al. 1999) was classified as a BLL by Schwobe et al. (2000), and as a HBL by Brinkmann et al. (2000). No previous optical spectroscopy was published. The VLT spectrum is featureless, with $\text{EW}_{\text{min}} = 1.27 \text{ \AA}$, which implies $z > 0.41$.

PKS 0823–223. This radio-selected BLL (Allen et al. 1982) is characterized by a number of absorption lines in the UV and optical band (e.g., Rao & Turnshek 2000; Meiring et al. 2007; Falomo 1990; Veron et al. 1990; Falomo et al. 1994). These features are consistent with the presence of a subdamped

$\text{Ly}\alpha$ (sub-DLA) absorber at $z = 0.91$. In our VLT spectrum we detect the absorption features of Fe II $\lambda\lambda 2373.7, 2383.2, 2585.9, 2599.4$, Mg II $\lambda 2798$, and Mg I $\lambda 2852$ at the same redshift.

PKS 1057–79. This radio-selected object (Shimmins & Bolton 1981) was proposed as a counterpart for the γ -ray source 2EGS 1050–7650 by Tornikoski et al. (2002). No previous optical spectroscopy was published. Our VLT spectrum shows several emission lines ([O III] $\lambda\lambda 4959, 5007$, [Ne III] $\lambda 3868$, Mg II $\lambda 2798$), at $z = 0.581$. Since the FWHM of the Mg II line (see Table 3) is in excess of 1000 km s^{-1} we propose to classify this object as a broad-line active galactic nucleus (AGN).

PKS 1145–676. This radio source was classified as a quasar due to its point-like appearance by White et al. (1987). The flat radio spectrum and optical variability (Beasley et al. 1997; Costa 2002) prompted a blazar classification. We detect several

emission lines ([O II] $\lambda 3727$, H β $\lambda 4861$, [O III] $\lambda \lambda 4959, 5007$, H α $\lambda 6563$, [N II] $\lambda 6585$) at $z = 0.210$. The observed EW are in the range 4–25 Å, pointing towards a FSRQ classification. The FWHM of the H β line could indicate that this source is a narrow lines object, but the fact that we are unable to measure the H α FWHM due to the blending with the [N II] lines permits only a type ~ 1.9 classification.

OM 280. This radio-selected source (Colla et al. 1972) was classified as a BLL due to its featureless spectrum by Strittmatter et al. (1974). Subsequent optical spectroscopy by Rector & Stocke (2001) also failed to discover any intrinsic spectral feature. The host galaxy was not detected in deep *Hubble Space Telescope* imaging (Urry et al. 2000), implying $z > 0.63$ (Sbarufatti et al. 2005a). The VLT spectrum is featureless, with $EW_{\min} = 0.35$ Å, which implies a redshift lower limit of 0.20, less stringent than the one from imaging.

PMN J1323–3652. This radio-selected source was classified as a candidate BLL by the WGA catalog (White et al. 2000) and the Deep X-ray Radio Blazar Survey (DXRBS, Landt et al. 2001) that also provided a featureless optical spectrum. However, our VLT optical spectrum clearly shows the absorption lines and the characteristic shape of a Galactic F-type star. This indicates a misidentification of the optical counterpart of this source.

OQ 012. This radio-selected BLL (Weiler & Johnston 1980) showed a featureless optical spectrum in observations by Falomo et al. (1994). Richards et al. (2004) gave a photometric redshift estimate $z = 0.475$ based on data from the Sloan Digital Sky Survey (SDSS). Our VLT spectrum shows an absorption line by Galactic ISM (Na I $\lambda 5891$), but no intrinsic features. The EW_{\min} is 0.31 Å, which implies $z > 0.65$, inconsistent with the photometric estimate.

PMNJ 1539–0658. This radio source (Griffith et al. 1995) was classified as a BLL in the DXRBS (Landt et al. 2001), which also provided a featureless optical spectrum. In the VLT spectrum we detect the Na I $\lambda 5891$ absorption line from the Galaxy, but no intrinsic features. The minimum detectable EW is 0.61 Å, which implies $z > 0.80$.

PKS 1830–589. This radio-selected BLL (Griffith et al. 1995; Landt et al. 2001) showed a featureless optical spectrum when observed in the DXRBS. Our VLT spectrum is also featureless (Na I $\lambda 5891$ is marginally detected with $EW = 0.4$ Å). The minimum detectable equivalent width is $EW_{\min} = 0.46$ Å, which gives a lower limit $z > 0.45$.

RBS 1752. This X-ray-selected BLL (Voges et al. 1999) had a tentative redshift $z = 0.449$ proposed in the Sedentary Survey (Giommi et al. 2005a; Piranomonte et al. 2007), based on the possible detection of the host galaxy spectral features in an ESO 3.6 m optical spectrum. The high S/N obtained using VLT allowed us to detect some weak host galaxy lines (Ca II $\lambda \lambda 3934, 3968$, *G* band $\lambda 4305$, and Mg I $\lambda 5175$) at $z = 0.449$. However, the *G* band is possibly contaminated by the [O I] atmospheric line at 6300 Å, and the Mg I line is very close to the telluric O₂ A band. Therefore, while the absorption features reported by Piranomonte et al. (2007) are confirmed, the redshift remains tentative because of the lack of other firm absorption features. The fit to the spectrum with a power-law plus elliptical galaxy model gives $M_R^{\text{host}} = -23.3$, in good agreement with the expected distribution $M_R^{\text{host}} = -22.9 \pm 0.5$.

RBS 1915. This X-ray-selected object (Voges et al. 1999) was classified as a BLL by Schwobe et al. (2000). The optical spectrum reported by Chavushyan et al. (2000) was featureless. Our VLT spectrum shows faint absorption lines from the BLL

host galaxy (Ca II $\lambda \lambda 3934, 3968$, *G* band $\lambda 4305$, and Mg I $\lambda 5175$) at $z = 0.243$. We performed a fit to the spectrum using a power-law plus elliptical galaxy model, obtaining $M_R^{\text{host}} = -22.4$, consistent with the expected distribution ($M_R^{\text{host}} = -22.9 \pm 0.5$).

TXS 2346+052. This radio-selected source (Large et al. 1981) was classified as a BLL because of its flat radio spectrum (Gorshkov et al. 2000) and the featureless optical spectrum (Chavushyan et al. 2000). Our VLT spectrum shows several emission lines (Mg II $\lambda 2798$, [O II] $\lambda 3727$, [Ne III] $\lambda 3868$, [O III] $\lambda \lambda 4959, 5007$) at $z = 0.419$. The observed EW of the Mg II and [O III] lines (exceeding 5 Å), rules out a BL Lac classification and suggests a FSRQ nature for this source. The EW ratio between the [O II] and [O III] lines are untypical for an AGN, possibly indicating an ongoing star formation (as seen in PKS 2005–489 by Bressan et al. 2006). A measurement of the equivalent width of the H α + [N II] line system (which is out of the observed spectral range) could help us to clarify this issue.

1RXS J235730.1–171801. This X-ray-selected object (Voges et al. 1999) was classified as a BLL by Schwobe et al. (2000). Our previous VLT observations (S06) gave a limit $z > 0.85$. The spectrum presented here has a slightly lower S/N (110, to be compared with 150 of the earlier observation, because of the different seeing conditions between the observations), that gives $EW_{\min} = 0.22$ Å and $z > 0.60$. Ca II $\lambda 3934$ and Na I $\lambda 5891$ absorptions from the Galaxy ISM are marginally detected (they were also detected in the S06 spectrum, along with several DIBs). No significant flux variations were detected between two different observation periods.

4. SUMMARY AND CONCLUSIONS

Of the 15 observed objects, we confirm the BL Lac classification for 11 sources, and the detection of a sub-DLA system in PKS 0823–223 ($z \geq 0.911$). PKS 1145–676 and TXS2346+052 are reclassified as FSRQ ($z = 0.210$ and $z = 0.419$, respectively), while PMN J1323–3652 is a F-type star. For three BLLs we are able to give a new determination of the redshift (PKS 1057–79, $z = 0.569$; RBS 1752, $z = 0.448$; RBS 1915, $z = 0.243$). For the remaining eight BLLs, we give redshift lower limits based on the minimum detectable equivalent width of their featureless spectra. On the whole, our BL Lac spectroscopy database now contains 45 confirmed BLLs observed with VLT, with 20 redshifts determined by the detection of faint lines, and 25 redshift lower limits.

In those cases where even VLT+FORs observations are inconclusive, a further increase in the S/N is required, for example through the use of adaptive optics, Very Large Telescope Interferometry, the Large Binocular Telescope, observations in the near-IR region, where the nucleus-to-host ratio is smaller than in the optical range, or, in the future, even the use of Extremely Large Telescopes. Alternatively, it would be possible to observe these sources when the active nucleus goes into a low state, since the decrease in the N/H ratio would make easier to detect the features of the host galaxy.

Based on observations collected at the European Organisation for Astronomical Research in the Southern Hemisphere, Chile. Observing proposal: ESO 077.B-0045 (PI: S. Ciprini). S.C. acknowledges the funding by the European Community's Human Potential Programme under contract HPRN-CT-2002-00321.

REFERENCES

- Abraham, R. G., Crawford, C. S., & McHardy, I. M. 1991, *MNRAS*, **252**, 482
- Allen, D. A., Ward, M. J., & Hyland, A. R. 1982, *MNRAS*, **199**, 969
- Bauer, F. E., Condon, J. J., Thuan, T. X., & Broderick, J. J. 2000, *VizieR Online Data Catalog*, **212**, 90547
- Beasley, A. J., Conway, J. E., Booth, R. S., Nyman, L.-A., & Holdaway, M. 1997, *A&AS*, **124**, 469
- Bressan, A., Falomo, R., Valdés, J. R., & Rampazzo, R. 2006, *ApJ*, **645**, L101
- Brinkmann, W., et al. 2000, *A&A*, **356**, 445
- Cardelli, J. A., Clayton, G. C., & Mathis, J. S. 1989, *ApJ*, **345**, 245
- Chavushyan, V., Mujica, R., Gorshkov, A. G., Konnikova, V. K., & Mingaliev, M. G. 2000, *Astron. Lett.*, **26**, 339
- Chen, P. S., Fu, H. W., & Gao, Y. F. 2005, *New Astron.*, **11**, 27
- Ciprini, S., Tosti, G., Teräsanta, H., & Aller, H. D. 2004, *MNRAS*, **348**, 1379
- Ciprini, S., et al. 2003, *A&A*, **400**, 487
- Colla, G., et al. 1972, *A&AS*, **7**, 1
- Condon, J. J., & Jauncey, D. L. 1974, *AJ*, **79**, 1220
- Costa, E. 2002, *A&A*, **381**, 13
- Davis, M. M. 1971, *AJ*, **76**, 980
- della Ceca, R., et al. 1990, *ApJS*, **72**, 471
- Donato, D., Ghisellini, G., Tagliaferri, G., & Fossati, G. 2001, *A&A*, **375**, 739
- Edwards, P. G., & Tingay, S. J. 2004, *A&A*, **424**, 91
- Falomo, R. 1990, *ApJ*, **353**, 114
- Falomo, R. 1996, *MNRAS*, **283**, 241
- Falomo, R., Scarpa, R., & Bersanelli, M. 1994, *ApJS*, **93**, 125
- Finke, J. D., Shields, J. C., Böttcher, M., & Basu, S. 2008, *A&A*, **477**, 513
- Flesch, E., & Hardcastle, M. J. 2004, *A&A*, **427**, 387
- Fricke, K. J., Kollatschny, W., & Witzel, A. 1983, *A&A*, **117**, 60
- Ghosh, K. K., & Soundararajaperumal, S. 1995, *ApJS*, **100**, 37
- Giommi, P., Piranomonte, S., Perri, M., & Padovani, P. 2005a, *A&A*, **434**, 385
- Giommi, P., Piranomonte, S., Perri, M., & Padovani, P. 2005b, *VizieR Online Data Catalog*, **343**, 40385
- Gorshkov, A. G., Konnikova, V. K., & Mingaliev, M. G. 2000, *Astron. Rep.*, **44**, 353
- Griffith, M. R., Wright, A. E., Burke, B. F., & Ekers, R. D. 1995, *ApJS*, **97**, 347
- Healey, S. E., et al. 2008, *ApJS*, **175**, 97
- Horne, K. 1986, *PASP*, **98**, 609
- Katajainen, S., et al. 2000, *A&AS*, **143**, 357
- Kinney, A. L., et al. 1996, *ApJ*, **467**, 38
- Landt, H., et al. 2001, *MNRAS*, **323**, 757
- Large, M. I., Mills, B. Y., Little, A. G., Crawford, D. F., & Sutton, J. M. 1981, *MNRAS*, **194**, 693
- Meiring, J. D., et al. 2007, *MNRAS*, **376**, 557
- Nass, P., et al. 1996, *A&A*, **309**, 419
- Nieppola, E., Tornikoski, M., & Valtaoja, E. 2006, *A&A*, **445**, 441
- Nilsson, K., et al. 2003, *A&A*, **400**, 95
- Oke, J. B. 1990, *AJ*, **99**, 1621
- Owen, F. N., & Muffson, S. L. 1977, *AJ*, **82**, 776
- Padovani, P., & Giommi, P. 1995, *ApJ*, **444**, 567
- Piranomonte, S., Perri, M., Giommi, P., Landt, H., & Padovani, P. 2007, *A&A*, **470**, 787
- Rao, S. M., & Turnshek, D. A. 2000, *ApJS*, **130**, 1
- Rector, T. A., & Stocke, J. T. 2001, *AJ*, **122**, 565
- Richards, G. T., et al. 2004, *ApJS*, **155**, 257
- Sbarufatti, B., Falomo, R., Treves, A., & Kotilainen, J. 2006a, *A&A*, **457**, 35
- Sbarufatti, B., Treves, A., & Falomo, R. 2005a, *ApJ*, **635**, 173
- Sbarufatti, B., et al. 2005b, *AJ*, **129**, 559
- Sbarufatti, B., et al. 2006b, *AJ*, **132**, 1
- Schlegel, D. J., Finkbeiner, D. P., & Davis, M. 1998, *ApJ*, **500**, 525
- Schwöpe, A., et al. 2000, *Astron. Nachr.*, **321**, 1
- Shimmins, A. J., & Bolton, J. G. 1981, *Aust. J. Phys.*, **34**, 471
- Strittmatter, P. A., Carswell, R. F., Gilbert, G., & Burbidge, E. M. 1974, *ApJ*, **190**, 509
- Tody, D. 1986, in *SPIE Conf. 627, Instrumentation in Astronomy VI: Proc. Meeting*, ed. D. L. Crawford (Bellingham, WA: SPIE), **733**
- Tody, D. 1993, in *ASP Conf. Ser. 52, Astronomical Data Analysis Software and Systems II*, ed. R. J. Hanisch, R. J. V. Brissenden, & J. Barnes (San Francisco, CA: ASP), **173**
- Tornikoski, M., Lähteenmäki, A., Lainela, M., & Valtaoja, E. 2002, *ApJ*, **579**, 136
- Urry, C. M., et al. 2000, *ApJ*, **532**, 816
- Veron, P., et al. 1990, *A&AS*, **86**, 543
- Voges, W., et al. 1999, *A&A*, **349**, 389
- Vollmer, B., et al. 2005, *A&A*, **431**, 1177
- Weiler, K. W., & Johnston, K. J. 1980, *MNRAS*, **190**, 269
- White, G. L. 1992, *Proc. Astron. Soc. Aust.*, **10**, 140
- White, G. L., Batty, M. J., Bunton, J. D., Brown, D. R., & Corben, J. B. 1987, *MNRAS*, **227**, 705
- White, N. E., Giommi, P., & Angelini, L. 2000, *VizieR Online Data Catalog*, **9031.0**
- Wills, B. J., & Wills, D. 1979, *ApJS*, **41**, 689
- Wright, S. C., McHardy, I. M., Abraham, R. G., & Crawford, C. S. 1998, *MNRAS*, **296**, 961
- Wu, Z., Jiang, D. R., Gu, M., & Liu, Y. 2007, *A&A*, **466**, 63